INTERFACE

royalsocietypublishing.org/journal/rsif

Research

Cite this article: Tegar S, Brass DP, Purse BV, Cobbold CA, White SM. 2026 Temperature-sensitive incubation, transmissibility and risk of *Aedes albopictus*-borne chikungunya virus in Europe. *J. R. Soc. Interface* **23**: 20250707.
https://doi.org/10.1098/rsif.2025.0707

Received: 11 July 2025
Accepted: 4 December 2025

Subject Category:
Life Sciences–Mathematics interface

Subject Areas:
biomathematics

Keywords:
autochthonous transmission, mechanistic model, basic reproduction number, thermal response curves, extrinsic incubation period, vector competence, arbovirus risk, climate suitability

Author for correspondence:
Sandeep Tegar
e-mails: s.tegar.1@research.gla.ac.uk; santeg@ceh.ac.uk

Electronic supplementary material is available online at https://doi.org/10.6084/m9.figshare.c.8230348.

THE ROYAL SOCIETY PUBLISHING

Temperature-sensitive incubation, transmissibility and risk of *Aedes albopictus*-borne chikungunya virus in Europe

Sandeep Tegar[1,2], Dominic P. Brass[1], Bethan V. Purse[1], Christina A. Cobbold[2] and Steven M. White[1]

[1]UK Centre for Ecology & Hydrology, Benson Lane, Wallingford, Oxfordshire, UK
[2]School of Mathematics and Statistics, College of Science and Engineering, University of Glasgow, Glasgow, UK

ST, 0009-0003-2445-9860; DPB, 0000-0002-4900-9124; BVP, 0000-0001-5140-2710; CAC, 0000-0001-8814-7688; SMW, 0000-0002-3192-9969

Chikungunya virus (CHIKV) has been reported in over 10 European countries. Despite the temperature sensitivity of mosquito-borne viruses, there are no specific models describing the temperature–trait relationship for the extrinsic incubation period (EIP) and vector competence (VC) of CHIKV within *Aedes albopictus*. This limits our understanding of how temperature influences CHIKV transmission risk in Europe. We used trait data obtained from a Preferred Reporting Items for Systematic Reviews and Meta-Analyses (PRISMA)-guided literature review to model the temperature–trait relationships for EIP and VC. These relationships were then integrated into a temperature-dependent basic reproduction number, $R_0(T)$, to generate climate-based risk maps and seasonal suitability. We estimate a maximum EIP_{50} of 8.7 days at 18°C, a minimum of 1.7 days at 30°C. The vector competence range spans 13.8–31.8°C, peaking at 25.6°C. Moreover, CHIKV is transmissible at lower temperatures than previously recognized, suggesting plausible transmission across most of Europe in July and August, with extended suitability from May to November in southern regions. CHIKV transmission is possible across a broad thermal range, placing large parts of Europe at risk—especially southern regions. Understanding which transmission areas receive the most incursions from trade and tourism during this period can further delineate risk areas for management.

1. Introduction

The global incidence of *Aedes*-borne arboviruses (arthropod-borne viruses), such as dengue, chikungunya and Zika, is increasing [1,2]. Chikungunya is an arthritogenic (leading to severe arthritis and joint pain) disease caused by the chikungunya virus (CHIKV), an *Alphavirus* in the family Togaviridae [3]. The first known outbreak of CHIKV was reported in Tanzania in 1952, and the virus currently affects public health in over 110 countries across Asia, Africa, Europe and the Americas [4]. As of November 8, 2024, approximately 480 000 cases of CHIKV and 190 deaths have been reported worldwide, affecting 23 countries [5].

Although chikungunya is not currently endemic in Europe, recent autochthonous outbreaks have been linked to the establishment of *Aedes albopictus* and cases introduced by viraemic travellers [5]. Since its introduction to southern Europe, detected in 2007, *Ae. albopictus* has spread to central and northern regions and is now the primary vector of CHIKV in Europe

[6]. The first locally transmitted chikungunya outbreak in Europe occurred in Italy in 2007, followed by several sporadic events, including major outbreaks in Italy and France in 2017 [5,7]. More recently, as of November 2024, a locally acquired case has been reported in mainland France [8]. Niche models driven by future climate projections suggest that the spread of *Ae. albopictus* into northern regions of Europe will continue, with a high likelihood of establishment across most of the continent [9], thereby increasing the potential for CHIKV transmission. Consequently, understanding the risk of autochthonous CHIKV transmission as temperature becomes more favourable for mosquito and virus activity is critically important for risk management [10,11].

The impact of temperature on CHIKV transmission by *Ae. albopictus* is poorly understood, mainly because of a knowledge gap in how temperature affects the extrinsic incubation period (EIP), vector competence (VC) and is linked to the risk of CHIKV spread across different regions, especially in recently invaded temperate zones [12]. Following ingestion of infected blood, EIP refers to the average time it takes for the virus to disseminate from the mosquito's midgut to its saliva, while VC is the proportion of mosquitoes with the virus in their saliva relative to those infected in the midgut [13]. As mosquitoes are ectotherms [14], temperature can have opposing, non-linear effects on mosquito survival and the EIP. However, there is no consensus as to how temperature limits the EIP of CHIKV. Some previous predictions of CHIKV spread, which assume a temperature-independent EIP (generally considered fixed values between 3 and 14 days [15–18]) are likely to bemisleading when predicting transmission risk near extreme temperature limits of mosquito survival, which is critical for mosquito-borne diseases (MBDs) in temperate zones. On the other hand, studies predicting CHIKV transmission risk using the EIP temperature–trait relationship derived from dengue virus (DENV) in *Aedes* mosquitoes [19–21] show considerable variability in the predicted temperature range suitable for CHIKV transmission [20,21]. This variability probably stems from biological differences in how CHIKV and DENV interact with *Aedes* mosquitoes. Empirical studies demonstrate considerable differences in the EIP and VC of CHIKV and DENV when transmitted by *Ae. aegypti* and *Ae. albopictus* [22,23]. As a result, using DENV- or *Ae. aegypti*-based traits to assess the risk of CHIKV transmission by *Ae. albopictus* may lead to misleading predictions.

Recently, mechanistic approaches have been developed for modelling temperature-sensitive transmission risks arising from exclusive virus–mosquito pairs [20,24–28]. These approaches are applied to quantify temperature-sensitive transmission risk on temporal and spatial scales for many MBDs and depend on the temperature–trait relationships (exclusive to virus–mosquito pair), such as mosquito development rate (MDR)—the rate at which mosquitoes progress from egg to adult—the probability of adult survival (survival probability), the biting rate (frequency of biting human hosts), the average number of eggs laid per female per day (fecundity), adult lifespan, VC and EIP [27]. These mechanistic models [20,24–27] have been successful at capturing the impact of temperature-sensitive variations in virus–mosquito traits and provide robust estimations of transmission risk but require extensive species-specific experimental data and high-computational power. However, owing to the lack of temperature–trait relationships for EIP and VC in CHIKV transmission by *Ae. albopictus*, no mechanistic models are available to assess the risk of CHIKV spread by this vector, which is crucial for studying the emerging transmission of CHIKV in Europe.

In this study, we conduct an extensive scoping literature review to determine the critical temperature–trait relationships for EIP and VC for CHIKV–*Ae. albopictus*, integrating empirical data across different geographical contexts and populations worldwide within this vector species. Furthermore, we incorporate these environment–trait relationships with an existing mechanistic model for the basic reproduction number ($R_0(T)$) [27] to study the impact of temperature on the transmission risk of *Ae. albopictus*-borne CHIKV spread in Europe. Through the $R_0(T)$ model, we identify the temperature range and seasons suitable for chikungunya transmission and map the current geographical limits of climate-driven transmission risk of CHIKV by *Ae. albopictus* across Europe. We consider the uncertainty and value of the model outputs for public health decision-making.

2. Methods

2.1. Literature search

We conducted an extensive scoping literature search to gather data on the effect of temperature on the EIP and VC for the combination of CHIKV and *Ae. albopictus*. We searched PubMed [29] and Scopus [30] from 1952 to April 15, 2025, using the terms 'CHIKV', 'chikungunya', 'albopictus', 'aegypti', 'vector', 'competence', 'dissemination' and 'transmission', without applying any language restrictions.

2.2. Review methodology and data collection

We followed the Preferred Reporting Items for Systematic Reviews and Meta-Analyses (PRISMA) methodology for the literature review. Documents obtained from PubMed and Scopus searches were processed using EndNote (EndNote 21). First, the search results for each query were saved in separate EndNote libraries and duplicates were removed. Then, all libraries were merged, and duplicates were removed again. The retrieved documents were then reviewed in three stages following PRISMA guidelines: by titles, abstracts and full texts (electronic supplementary material, figure S1) [31]. We defined selection criteria (see electronic supplementary material, section S1) to identify relevant studies available online and recorded the data in a spreadsheet, including resource DOI, vector (*Ae. albopictus*), vector geographical location, location type, vector genotype, vector strain, vector generation, virus (CHIKV), virus geographic location, virus genotype, virus strain, dose of virus fed to mosquitoes, dose unit, type of laboratory test, sample size, temperature, temperature unit, humidity, humidity unit, days post-infection (dpi), dissemination proportion, dissemination definition, transmission proportion and transmission definition. In our literature review, we primarily focused on studies reporting the detection of CHIKV particles at least in the salivary glands of *Ae. albopictus* mosquitoes, which we define as indicative of a transmissible infection in the mosquito.

2.3. Statistical analysis

All regression analyses were performed using Bayesian regression, implemented with the 'R2jags' package in R (version 4.4.1) [32]. Model comparisons were conducted using deviance information criteria (DIC), mean deviance (MD) and widely applicable information criterion (WAIC) scores, calculated using 'R2jags'. Additionally, the 'HDInterval' package in R was used to compute 95% credible intervals (i.e. 95% CI or the 95% highest density intervals (HDI)) [33].

2.4. Modelling the relationship between days post-infection and infectious proportion

For a given experimental temperature and dpi, we define the infectious proportion as the ratio of mosquitoes with a detectable infection in at least the salivary glands to the total number of exposed mosquitoes (i.e. those that fed on CHIKV-infected blood). Studies suggest that the infectious proportion should follow an increasing S-shaped relationship (i.e. sigmoidal function) with dpi [13]. Therefore, for each experimental temperature of 18, 20, 22, 26, 27, 28 and 30°C, we have used three models (Logistic, Gompertz and Hill) to capture the S-shaped relationship (table 1). At each temperature, the best-fit model was selected based on its overall performance across three metrics: DIC, WAIC and MD. The model that performed best across most temperature values was then chosen as the overall best model. However, model selection is relative and should not be interpreted in absolute terms. Therefore, we additionally estimated the temperature responses of the transmission risk of CHIKV (i.e. $R_0(T)$) across all combinations of EIP and VC models and metrics to assess their impact on the overall results (electronic supplementary material, section S5).

2.5. Estimating vector competence, extrinsic incubation period and parasite development rate

For each experimental temperature of 18, 20, 22, 26, 27, 28 and 30°C vector competence ($VC_{max}(T)$) is defined as the asymptote of the sigmoidal function fitted to the infectious proportion as a function of dpi, we also estimate $VC_{50}(T)$, defined as 50% of the asymptote value. In the remainder of this paper, VC refers to $VC_{max}(T)$, unless $VC_{50}(T)$ is specifically mentioned. We have defined three metrics of the extrinsic incubation periods, i.e. $EIP_n(T)$ (for $n = 10, 50$ and 90), to be the value of dpi at which n% of $VC_{max}(T)$ is reached [13]. Specifically, $EIP_{50}(T)$ is the dpi at which 50% of the maximum vector competence (i.e. $VC_{50}(T)$) is achieved. The posteriors of the parameters obtained from the model fits of infectious proportions as a function of dpi are used to estimate the posterior distributions of each $EIP_n(T)$, and then, for each $n = 10$, 50 and 90, the posterior distributions for parasite development rates, $PDR_n(T)$, are obtained by taking the reciprocal of the posteriors of $EIP_n(T)$ [20,24]. Finally, for each experimental temperature value T, we calculated the mean, median and 95% CI from the posterior distributions of $VC_{max}(T)$, $VC_{50}(T)$, $EIP_n(T)$ and $PDR_n(T)$. In the further analysis, we used these posterior medians as the representative values of $VC_{max}(T)$, $VC_{50}(T)$, $EIP_n(T)$ and $PDR_n(T)$ at each experimental temperature value T, with variability around the fitted medians indicated by the corresponding 95% CI.

2.6. Fitting the relationships between temperature and extrinsic incubation period, parasite development rate and vector competence

To model the relationship between temperature and EIP_n, we fitted a degree–day model, an exponential model and the model proposed to study the temperature response of ontogenetic development time (we refer to it as the development time model, DTM, for convenience in the rest of the paper) [39]. The DTM is used to fit embryonic development times for a wide range of incubation temperatures for aquatic ectotherms, including insects [39,40]. The temperature dependence of PDR_n was modelled by fitting the Brière model, a linear model and the development rate model (DRM), equivalent to the reciprocal of DTM (see table 1). Finally, the temperature–trait relationships for VC_{max} and VC_{50} were modelled using a commonly used functional form, i.e. quadratic function (table 1) [27]. We set the variance of priors wide enough to encompass the 95% credible intervals (CIs) around the median data points for each temperature value while fitting the models.

2.7. Temperature-sensitive basic reproduction number ($R_0(T)$)

Mechanistic $R_0(T)$ models have commonly been used to study the temperature sensitivity of MBDs [20,24–27,41]. These models provide a metric for assessing the impact of mosquito ecology and virus epidemiology within a risk assessment framework. At a given temperature T, $R_0(T)$ is the average number of new infections generated by an infectious human or mosquito, in either host class, per transmission generation [42]. In this approach, the temperature responses of traits belonging to a specific mosquito–virus combination are incorporated into a common expression of R_0 [43], thereby defining $R_0(T)$ for that specific mosquito–virus pair. To achieve this for *Ae. albopictus*–CHIKV, we modelled the thermal responses of traits: PDR and VC, for CHIKV in combination with *Ae. albopictus*. Additionally, we incorporated the thermal responses of the following traits for *Ae. albopictus* from an existing study: egg-to-adult development rate (MDR), egg-to-adult survival probability (p_{EA}), fecundity (eggs per female per day; EFD), biting rate (a) and adult mosquito mortality rate (μ) or adult life span ($1/\mu$) (electronic supplementary material, figure S22) [20]. This results in the following temperature-sensitive $R_0(T)$ for the transmission of CHIKV by *Ae. albopictus*:

Table 1. List of models used to fit the relationship between dpi and infectious proportion (IP), as well as the thermal responses of EIPs, parasite development rates (PDRs) and VCs. Fitted model parameter values and prior distributions are provided in the electronic supplementary material, tables S1, S5, S7, S9 and S10. For the derivation of EIP_n and PDR_n from the expressions for $\mathrm{EIP}(T)$ and $\mathrm{PDR}(T)$ given in this table, see the electronic supplementary material, section S3.

models	expression	references
logistic model	$\mathrm{IP} = VC/(1+\exp(-k(dpi-d_{50})))$	[34]
Gompertz model	$\mathrm{IP} = \mathrm{VC}\exp(-\exp(-k(dpi-d_{50})))$	[35]
Hill equation	$\mathrm{IP} = \left(VC\,dpi^k\right)/\left(d_{50}^k + dpi^k\right)$	[36]
degree-day model (DDM)	$\mathrm{EIP}(T) = D/(T-T_{min})$	[37]
exponential model	$\mathrm{EIP}(T) = \exp\left(\beta_0 + \beta_T T + \frac{1}{2\tau}\right)$	[38]
development time model (DTM)	$\mathrm{EIP}(T) = A\exp\left(-k\left(\frac{T}{1+T/273}\right)\right)$	[39]
linear model	$\mathrm{PDR}(T) = \alpha + \beta T$	reciprocal of DDM
Brière model	$\mathrm{PDR}(T) = qT(T-T_0)\sqrt{T_m - T}$	[20]
development rate model (DRM)	$\mathrm{PDR}(T) = B\exp\left(k\left(\frac{T}{1+T/273}\right)\right)$	reciprocal of DTM
quadratic model	$\mathrm{VC}(T) = -c(T-T_0)(T-T_m)$	[20]

$$R_0(T) = \sqrt{\frac{a(T)^2 b(T) c(T) e^{-\mu(T)/PDR(T)} \mathrm{EFD}(T) p_{EA}(T) \mathrm{MDR}(T)}{N r \mu(T)^3}},$$

where $b(T)c(T)$ represents VC; it is the product of the proportion of bites by infectious mosquitoes that infect healthy humans and the proportion of mosquitoes that become infected after biting an infectious human, N is the human density and r is the recovery rate of infected humans. For computing $R_0(T)$, we have used a commonly used metric of PDR, i.e. PDR_{50} (or $1/\mathrm{EIP}_{50}(T)$) [13,20] and corresponding vector competence, i.e. $\mathrm{VC}_{50}(T)$. We also compared the impact of using different combinations of models and metrics for the temperature–trait relationships of EIP, PDR and VC (see electronic supplementary material, section S5).

2.8. Spatial risk mapping and monthly risk analysis

A spatial risk map and monthly risk analysis for Europe are generated from the relative basic reproduction number, $R_{0r}(T)$, which, for optimum temperature T_{opt}, is given by the expression $R_{0r}(T) = R_0(T)/R_0(T_{opt})$. Here, the optimum temperature, T_{opt}, is the temperature value at which $R_0(T)$ attains its maximum value. In this case, the transmission threshold (i.e. $R_0(T) = 1$) becomes $R_{0r}(T) = 1/R_0(T_{opt})$. We used the relative R_{0r} instead of the standard R_0 to avoid incorporating the host-to-vector ratio for each pixel across Europe. Estimating the host-to-vector ratio at a given location is a highly challenging and complex task [44]. Consequently, human population density (N) is not included in the computation of the risk maps. For brevity, in the remainder of this paper, we will use standard notations [20,24,27], i.e. $R_0(T)$ and $R_0(T) > 1$, to refer to $R_{0r}(T)$ and the transmission condition $R_{0r}(T) > 1/R_0(T_{opt})$. Furthermore, to conduct the risk analysis, we have used hourly air temperature at 2 m above the land surface ('2 m temperature'), sourced from the ERA5-land climate reanalysis dataset [45]. This dataset covers the period from 2007 to 2023, with a spatial resolution of 0.1° × 0.1° (the native resolution is 9 km). The daily mean temperature is then calculated on the same spatio-temporal grid. Subsequently, $R_0(T)$ is computed at the daily mean temperature for each spatial grid cell. At this stage, we applied a 7 days rolling mean to the computed $R_0(T)$ to reduce noise and emphasize long-term trends in the risk. To derive the probabilities of monthly risk of CHIKV transmission, we first created a binary event dataset (with values 0 and 1) from the computed $R_0(T)$ dataset, where 0 corresponds to $R_0(T) \leq 1$ and 1 corresponds to $R_0(T) > 1$. For each grid cell, we then calculated the monthly average of the event dataset from 2007 to 2023 to estimate the probabilities $P(R_0(T) > 1)$ at a monthly resolution. Furthermore, to identify consecutive months where $P(R_0(T) > 1) \geq 0.95$, we created a new binary event dataset: assigning a value of 1 where $P(R_0(T) > 1) \geq 0.95$, and 0 otherwise. Using this binary dataset, we then counted the number of consecutive months by summing and overlapping (monthly) time windows for each grid cell (see electronic supplementary material, section S6 for the detailed computational methodology and electronic supplementary material, figures S28 and S29 for getting consecutive months by overlapping monthly maps). Here, a 95% probability threshold is chosen to capture only high-risk trends. To quantify the seasonality in each European country included in our study, we used bar diagrams. Each bar in the diagrams represents the proportion of grid cells with $P(R_0(T) > 1) \geq 0.95$, relative to the total number of grid cells within a country for each month of the year. These bar charts illustrate both the seasonal patterns and the spatial extent of areas at risk for each European country analysed in our study. For example, in the case of the United Kingdom, the bars indicate that approximately 15–20% of the geographical area is at risk during the months of July and August, and the associated map shows the specific areas at risk within the country (figure 1).

3. Results

3.1. Identification of literature

The five search strings yielded a total of 6515 documents, after removing duplicates from each search individually (electronic supplementary material, figure S1). When combining all search results into one library, 1805 documents remained after removing 4710 duplicates. Following a well-defined selection criterion (electronic supplementary material, section S1), title screening of the 1805 documents resulted in 297 selected documents. Abstract screening of the 297 documents resulted in 81 potential documents. Of these, 27 were excluded owing to methodological or data insufficiencies, and five were excluded because full-length articles were unavailable. Finally, 49 documents were included in the study. We found that experimental vector competence studies for CHIKV–*Ae. albopictus* were conducted at fixed temperatures of 15, 18, 20, 21, 22, 24, 25, 26, 27, 28 and 30°C. However, we excluded temperatures of 15, 21, 24 and 25°C from the modelling of the relationship between dpi and infectious proportions, as there was insufficient dpi data at these temperatures to establish a relationship. Additionally, we recorded the geographical location of *Ae. albopictus*, CHIKV lineage, various definitions of dissemination and transmission (or infectiousness) used in the literature, and sample sizes for improved modelling purposes. However, our modelling study used only temperature, dpi and infectious proportions, owing to insufficient data to model the effect of any additional variables on EIP or VC. A total of 405 data points were recorded from the selected documents in a spreadsheet [46].

3.2. Relationship between days post-infection and transmission proportions

The DIC, WAIC and MD scores for the Hill model are consistently better than those for the logistic and Gompertz models across most experimental temperatures, with the Hill model performing best at six of the seven temperature points (electronic supplementary material, table S2). Therefore, we selected the Hill model for subsequent analysis.

3.3. Estimates of extrinsic incubation period, parasite development rate and vector competence

For each of the experimental temperature values, EIP_n, PDR_n, VC_{max} and VC_{50} are estimated from the relationship between dpi and infectious proportion fitted using the Hill model (figure 2). The predicted values of EIP_n show a decreasing trend as temperature increases. EIP_n values decrease from, at 18°C, EIP_{10} = 7.11 days (95% credible interval (i.e. 95% CI): 5.21–12.37 days), EIP_{50} = 8.74 days (95% CI: 6.67–13.97 days) and EIP_{90} = 10.80 days (95% CI: 7.16–17.80 days) to at 30°C, EIP_{10} = 1.42 days (95% CI: 0.19–3.20 days), EIP_{50} = 1.74 days (95% CI: 0.24–3.79 days) and EIP_{90} = 2.08 days (95% CI: 0.25–4.44 days). In contrast, the predicted value of PDR_n shows an increasing trend with increasing temperature. At 18°C, PDR_{10} = 0.14 (95% CI: 0.08–0.19), PDR_{50} = 0.11 (95% CI: 0.07–0.15) and PDR_{90} = 0.09 (95% CI: 0.05–0.13), while at 30°C, PDR_{10} = 0.70 (95% CI: 0.22–2.40), PDR_{50} = 0.57 (95% CI: 0.20–1.99) and PDR_{90} = 0.48 (95% CI: 0.17–1.69). The predicted values of VC show a bell-shaped response to temperature, with the optimum competence (i.e. the maximum proportion of infectious mosquitoes) of VC_{max} = 0.96 (95% CI: 0.89–1.0) achieved at 22°C (table 2).

3.4. Thermal response of the extrinsic incubation period, parasite development rate and vector competence

We find that the thermal response curves of EIP_n are best represented by the degree–day model, while the Brière model is the most suitable for PDR_n (i.e. the reciprocal of EIP_n), and the quadratic model performs best for vector competence (VC_{max}) and also for VC_{50}. Among the $EIP_n(T)$ models, the degree–day model has the lowest WAIC and MD scores and the second-best-fitted model, DTM (the model of temperature dependence of the embryonic-development time proposed in Gillooly *et al.* [39]), achieves the minimum DIC score across all the EIP_n (electronic supplementary material, table S8). Despite its strong performance, the degree–day model has certain limitations and remains insufficiently validated [47]. Notably, its behaviour at lower temperatures relies heavily on extrapolation. For example, in our study, empirical measures of vector competence below 18°C are unavailable for estimating EIP_n. Therefore, the temperature response of EIP_n, as given by the degree–day model, cannot be extrapolated below 18°C, as the model breaks down near this temperature point due to division by zero. Consequently, we recommend using the DTM model, which gives a smooth and consistent temperature response of EIP_n below 18°C and provides mathematically tractable estimates of how temperature affects EIP_n across a biologically relevant range (figure 3). For PDR_n, the Brière model has the lowest scores across all three criteria: DIC, WAIC and MD tests—and was therefore used in the subsequent $R_0(T)$ analysis (electronic supplementary material, table S11).

3.5. Temperature sensitivity of chikungunya virus transmission by *Aedes albopictus*

The thermal response of $R_0(T)$ exhibits a unimodal and asymmetrical relationship with temperature. The posterior distribution of $R_0(T)$, based on the thermal responses of PDR_{50} (Brière model) and VC_{50}, provides the following temperature range (defined by the minimum and maximum cut-off temperatures, T_{min} and T_{max}, respectively) suitable for the CHIKV transmission by *Ae. albopictus*: T_{min} = 13.84°C (95% CI: 10.7–17.4°C), T_{max} = 31.85°C (95% CI: 30–35.2°C), with the optimum temperature for CHIKV transmission by *Ae. albopictus* occurring at T_{opt} = 25.63°C (95% CI: 24.3–27°C) (figure 4). We compared the impact of using different combinations of models and metrics for the temperature–trait relationships of EIP, PDR and VC on $R_0(T)$ (electronic

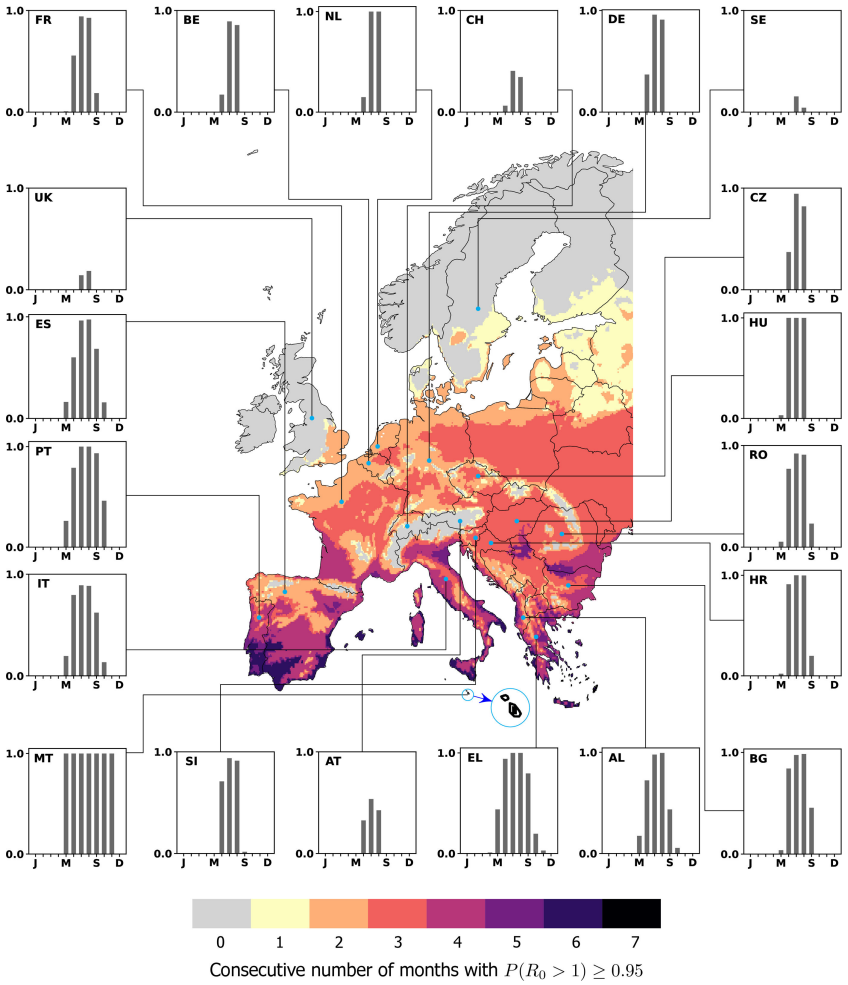

Figure 1. Map of predicted temperature suitability for CHIKV transmission by *Ae. albopictus* in Europe. Bar charts represent the seasonal risk of transmission in countries where *Ae. albopictus* is either established or introduced [6]. The y-axis on the bar charts represents the proportion of the geographical area of each country with a 95% probability of CHIKV transmission, i.e. $P(R_0(T) > 1) \geq 0.95$, relative to the total area of the country, plotted by month. For seasonal trends in all EU/EEA countries, refer to the electronic supplementary material, figure S27. In the bar charts, the letters on the *x*-axis denote the months January (J), May (M), September (S) and December (D).

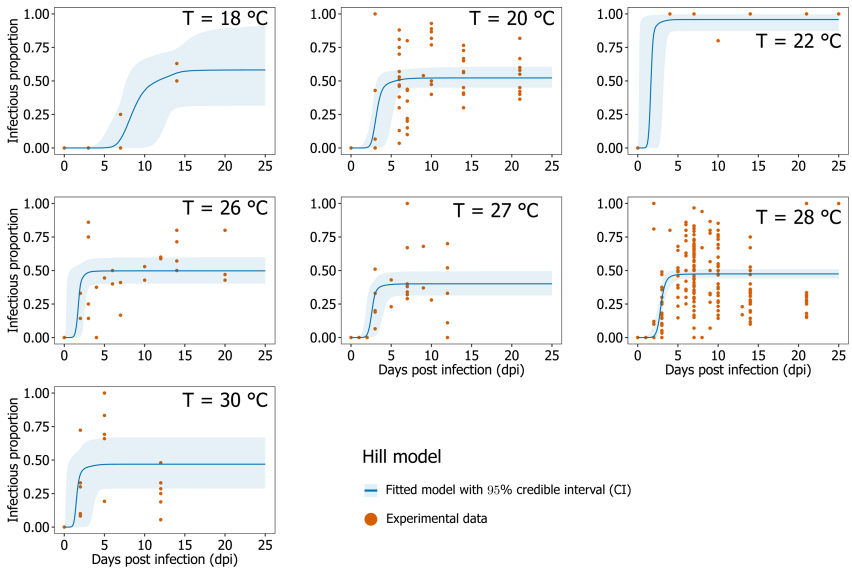

Figure 2. Fitted infectious proportion as a function of dpi using the Hill model. The solid line is the fitted median curve, the shaded band indicates the 95% CI (credible interval) and the points are the data. Corresponding fitted curves obtained using the logistic and Gompertz models are provided in the electronic supplementary material, figures S5 and S6.

supplementary material, section S5). However, no considerable impact on the thermal response of $R_0(T)$ was observed (electronic supplementary material, figures S23–S25).

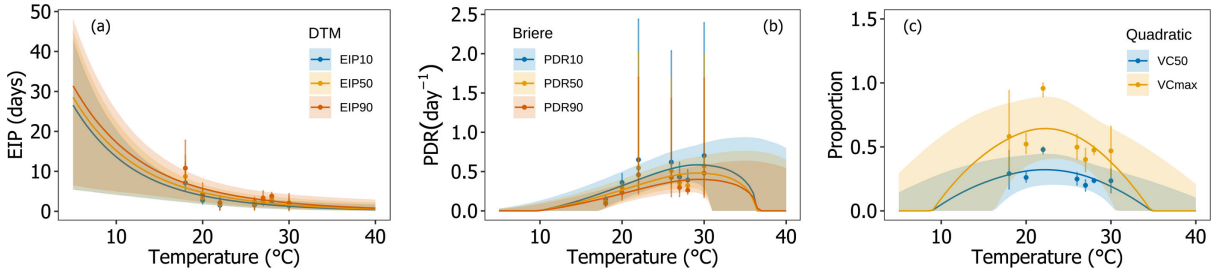

Figure 3. Fitted thermal response curves for EIP_n, PDR_n, VC_{max} and VC_{50}. The solid line is the fitted median curve, the shaded band indicates the 95% CI (credible interval), and the dots are the estimated values of EIP_n, PDR_n, VC_{max} and VC_{50}, as obtained from the Hill model of infectious proportion against dpi. Thermal response curves are as follows: (a) EIP_n –DTM model, (b) PDR_n –Brière model and (c) $VC_{max}$and VC_{50}–quadratic model. Corresponding fitted curves using alternative models are provided in the electronic supplementary material, figures S17 and S20.

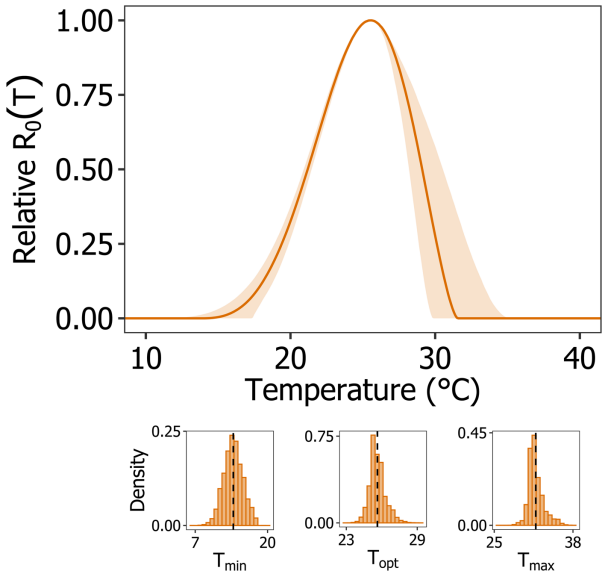

Figure 4. Relative $R_0(T)$ for CHIKV transmission by *Ae. albopictus*. The solid line is the fitted median curve, and the shaded band around it indicates the 95% CI (credible intervals). The bar charts at the bottom show the posterior distributions of the minimum (T_{min}) and maximum (T_{max}) cut-off temperatures and optimum transmission temperature (T_{opt}) for the CHIKV transmission by *Ae. albopictus*. The vertical dotted lines within the bar charts indicate the median of the corresponding distributions.

3.6. Risk of chikungunya virus transmission in Europe

Based on the thermal response of $R_0(T)$ for *Ae. albopictus* and CHIKV, transmission of CHIKV by *Ae. albopictus* is possible when the temperature remains within the critical range (13.84–31.85°C). Analysis of the average monthly transmission risk across Europe from 2007 to 2023 reveals that CHIKV transmission by *Ae. albopictus* is highly probable ($P(R_0(T) > 1) \geq 0.95$) from May to October, with the peak transmission occurring in July and August. Approximately 50% of Europe's geographical area is suitable for transmission during July and August (electronic supplementary material, figure S26). The risk gradient is higher in the southern parts of Europe, which decreases as one moves towards the north and northwest. Areas with the highest risk (i.e. $P(R_0(T) > 1) \geq 0.95$ for 6 or more months per year, from May to November) include Albania (AL), Greece (EL), Italy (IT), Malta (MT), Spain (ES) and Portugal (PT). Moderately risky zones (i.e. $P(R_0(T) > 1) \geq 0.95$ for 3–5 months per year, from May to September) are identified as Austria (AT), Belgium (BE), Bulgaria (BG), Croatia (HR), Czech Republic (CZ), France (FR), Germany (DE), Hungary (HU), Lithuania (LT), Luxembourg (LU), Netherlands (NL), Poland (PL), Romania (RO), Slovakia (SK), Slovenia (SI) and Switzerland (CH). Low-risk zones (i.e. $P(R_0(T) > 1) \geq 0.95$ for less than three months per year, including July and August) include Denmark (DK), Estonia (EE), Finland (FI), Ireland (IE), Latvia (LV), Liechtenstein (LI), Norway (NO), Sweden (SE) and the United Kingdom (UK) (figure 1).

4. Discussion

The instances of autochthonous *Aedes*-borne arboviral infections in Europe have been increasing at an average annual rate of 25%, with the southern European countries now experiencing recurring chikungunya and dengue outbreaks over the years [48]. Since mosquitoes are ectotherms [14], quantifying the temperature range and optimum operative temperature, based on temperature–transmission relationships, is essential for understanding the geographical distribution and seasonal patterns of MBDs [20,27]. Temperature–transmission relationships for *Ae. albopictus*–CHIKV have not been well defined, partly owing to data sparseness, but also because they have been extrapolated from other virus–mosquito pairs without accounting for well-parametrized temperature–trait relationships [12,16].

Table 2. Computed median values and 95% CIs (credible intervals) of EIP_n, PDR_n, VC_{50} and VC_{max} at fixed temperatures based on the Hill model. Corresponding values obtained using the logistic and Gompertz models are provided in the electronic supplementary material, tables S3 and S4.

temperature (°C)	EIP						PDR						VC			
	10%	CI	50%	CI	90%	CI	10%	CI	50%	CI	90%	CI	VC_{50}	CI	VC_{max}	CI
18	7.11	(5.21, 12.37)	8.74	(6.67, 13.97)	10.80	(7.16, 17.80)	0.14	(0.08, 0.19)	0.11	(0.07, 0.15)	0.09	(0.05, 0.13)	0.29	(0.17, 0.47)	0.58	(0.34, 0.94)
20	2.77	(1.83, 4.54)	3.39	(2.73, 5.43)	4.29	(3.10, 7.09)	0.36	(0.20, 0.47)	0.29	(0.18, 0.35)	0.23	(0.13, 0.31)	0.26	(0.22 0.30)	0.52	(0.45, 0.60)
22	1.54	(0.26, 2.99)	1.83	(0.31, 3.36)	2.18	(0.40, 3.92)	0.65	(0.28, 2.44)	0.55	(0.26, 2.02)	0.46	(0.21, 1.70)	0.48	(0.45, 0.50)	0.96	(0.89, 1.00)
26	1.61	(0.37, 2.46)	1.96	(0.47, 2.85)	2.34	(0.36, 3.53)	0.62	(0.36, 2.04)	0.51	(0.29, 1.69)	0.43	(0.18, 1.43)	0.25	(0.20, 0.30)	0.50	(0.40, 0.60)
27	2.32	(1.45, 3.23)	2.81	(1.84, 3.88)	3.35	(2.19, 5.13)	0.43	(0.27, 0.62)	0.36	(0.24, 0.50)	0.30	(0.18, 0.43)	0.20	(0.15, 0.24)	0.40	(0.31, 0.49)
28	2.54	(1.90, 2.91)	3.08	(2.80, 3.44)	3.80	(3.23, 4.72)	0.39	(0.34, 0.52)	0.32	(0.29, 0.36)	0.26	(0.21, 0.31)	0.24	(0.22, 0.25)	0.48	(0.44, 0.51)
30	1.42	(0.19, 3.20)	1.74	(0.24, 3.79)	2.09	(0.25, 4.44)	0.70	(0.22, 2.40)	0.57	(0.20, 1.99)	0.48	(0.17, 1.69)	0.23	(0.14, 0.33)	0.46	(0.28, 0.66)

This study provides a comprehensive estimation of the temperature–trait relationship for EIP and VC of CHIKV in *Ae. albopictus* across an epidemiologically relevant temperature range, by drawing on empirical data from 49 studies across the global range of these species. A mechanistic $R_0(T)$ model [27], based on these refined temperature–trait relationships, identifies the thermal range suitable for CHIKV transmission by *Ae. albopictus*, along with the corresponding predicted geographical distribution and seasonal patterns of chikungunya transmission in Europe.

Compared with previous studies on CHIKV transmission risk, which relied on estimates of temperature–trait relationships for EIP and VC based on dengue virus (DENV) studies [20,21], our research highlights the notable differences between temperature–trait relationships for EIPs and VCs between *Ae. albopictus*-borne CHIKV and DENV. For example, at 30°C, the mean EIP_{50} for DENV is 6.5 days (95% CI: 4.8–8.8 days) [49], whereas the predicted EIP_{50} for CHIKV in our study is much shorter at 1.78 days (95% CI: 0.24–3.79 days). Similarly, at 27°C, the empirical estimate of VC_{max} for DENV is 67% [50], compared with our prediction of 40% (95% CI: 31–49%) for CHIKV. Empirical studies contrasting these quantities for circulating DENV and CHIKV in the same *Ae. Albopictus* populations have found the EIP of CHIKV to be shorter than that of dengue [51,52] but have also found *Ae. albopictus* to be more competent for specific CHIKV genotypes (e.g. Reunion isolate (LR2006 OPY1) [23]) than dengue or other closely related CHIKV genotypes [53,54], though the biological basis of these differences in *Ae. albopictus* competence for different virus species and strains requires further study. Our prediction of the maximum cut-off temperature for CHIKV transmission (i.e. T_{max} = 31. 85°C (95% CI: 31–35.2°C)) is comparable with previous predictions [20,21]. However, our prediction of the minimum cut-off temperature (i.e. T_{min} = 13.84°C (95% CI: 10.7–17.4°C)) is approximately 2–2.5°C lower than earlier estimates (e.g. 16.2°C (95% CI: 13.3–19.9°C)). This difference is important for predicting chikungunya transmission risk in temperate zones and highlights the value of combining trait–environment data across populations for a more comprehensive assessment of risk areas.

The importance of selecting a specific EIP_n (i.e. n = 10, 50 or 90) for estimating the transmission risk of MBDs has been highlighted in previous studies [13,55]. To assess the impact of this choice, we estimated the temperature–transmission relationship (i.e. $R_0(T)$) using different PDR_n values (which are inversely proportional to EIP_n values), in combination with different PDR models (i.e. linear, Brière and the development rate model (DRM)). However, despite the slight differences in EIP_n (electronic supplementary material, figures S17 and S8), we observed that the choice of EIP_n (reflected by the choice of PDR_n) had no substantial impact on the temperature-dependent transmission risk as assessed by the mechanistic $R_0(T)$ model (electronic supplementary material, figures S23–S25). This can possibly be explained by the low sensitivity of $R_0(T)$ to variations in EIP [20]. In general, this can also be explained by Jensen's inequality [56,57], which helps clarify why the nonlinear thermal performance curves for EIP (or PDR), when estimated at fixed temperatures, can alter the perceived effects of temperature fluctuations on the temperature-dependent transmission risk, i.e. $R_0(T)$. On the other hand, in dynamically varying systems that produce time-varying estimates of transmission risk (e.g. effective reproduction number, R_t) [28], the temporal fluctuations in temperature can alter the generation time of infection (and consequently R_t) [58] by affecting the thermal performance curves for EIP, with the extent of these changes depending on the specific EIP metrics and models used.

Our $R_0(T)$ model indicates broad suitability for CHIKV transmission risk across Europe. Previous attempts to map this risk have drawbacks in their modelling approaches, which may lead to inaccuracies in their predictions. For example, previous maps assumed a shared temperature–trait relationship models for *Ae. aegypti* and *Ae. albopictus*, used the temperature–trait relationship models for dengue as a proxy for CHIKV [18,19], or assumed categorical or linear relationships between temper-

ature and transmission traits [16,17]. In contrast, our study captures the nonlinear relationship between temperature and transmission traits specifically for *Ae. albopictus* and CHIKV, enabling more accurate predictions of disease risk.

Using the EIP and VC temperature–trait relationships for CHIKV and *Ae. albopictus* in a transmission risk $R_0(T)$ model, our study suggests a higher climate suitability for chikungunya transmission in Europe compared with DENV [8]; however, the annual frequency of chikungunya outbreaks and their geographical spread are both lower compared with those of dengue on a global scale. This difference may be attributable to factors beyond generation times (EIP and intrinsic incubation period), including the diversity of epidemiologically significant serotypes and the nature of immunity conferred. Dengue virus (DENV) has four serotypes (with DENV-1 to DENV-3 reported in Europe), and infection provides only partial, serotype-specific immunity [59]. In contrast, CHIKV has a single serotype, and infection typically results in lifelong immunity [9,59]. Since chikungunya and dengue are most likely imported in Europe by viraemic travellers [60], the global distribution and prevalence of dengue and chikungunya, along with the timing, frequency and magnitude of travel between Europe and epidemic zones, are also critical factors that play a highly significant role in transmission risk, in addition to climate suitability for transmission.

The data of European Centre for Disease Prevention and Control (ECDC) indicate that CHIKV cases imported into Europe originate from regions endemic to all four major global lineages of CHIKV (e.g. ECSA, Asian, IOL and West African) [60]. Our extensive scoping literature review found insufficient data to model separate temperature–trait relationships for EIP and VC for each major CHIKV lineage. However, laboratory studies underline the importance of the temperature–trait relationship for biological processes, which can vary with the genetic and phenotypic diversity of viruses and mosquitoes [54,61]. For example, CHIKV transmission by *Ae. albopictus* depends on the combination of temperature and the genotypes of both *Ae. albopictus* and CHIKV [22,23,53,61]. In contrast to studies that overlook genotype-by-genotype-by-environment interactions, empirical studies emphasize the importance of considering the interplay between genotype and environment across both mosquitoes and viruses to accurately assess transmission risk [22,61]. Therefore, the possibility of autochthonous chikungunya transmission in Europe, driven by *Ae. albopictus* adapting to new CHIKV strains (or lineages) through travel from endemic regions, requires further investigations. This includes incorporating climate variables, trait differences in both viruses and mosquitoes and human population data into transmission models to better assess the epidemiological risk.

5. Conclusion

The temperature–transmission relationship, temperature range and seasonal patterns achieved for *Ae. albopictus* and chikungunya in our study are highly valuable for quantitative comparison with *Ae. albopictus*-borne diseases like dengue and Zika, which help design focused control strategies across Europe. Our results highlight that chikungunya transmission presents a broad risk across Europe, peaking in July and August, which may help with targeting future public health interventions. Leveraging sparse environment–trait data across virus and *Aedes* vector ranges to better estimate temperature–transmission relationships is fruitful for mapping transmission risk areas for *Aedes*-borne diseases in Europe, particularly as transmission parameters are resolved at virus strain and vector genotype level.

Ethics. This work did not require ethical approval from a human subject or animal welfare committee.

Data accessibility. All model code and supporting datasets used in this study are openly available on Zenodo [46]. The climate data (ERA5) used in this study are publicly available from the European Centre for Medium-Range Weather Forecasts (ECMWF) [62].

Supplementary material is available online [63].

Declaration of AI use. We have not used AI-assisted technologies in creating this article.

Authors' contributions. S.T.: conceptualization, data curation, formal analysis, investigation, methodology, software, validation, visualization, writing—original draft; D.B.: funding acquisition, supervision, writing—review and editing; B.V.P.: supervision, writing—review and editing; C.A.C.: funding acquisition, supervision, writing—review and editing; S.M.W.: conceptualization, funding acquisition, project administration, resources, supervision, validation, writing—review and editing.

All authors gave final approval for publication and agreed to be held accountable for the work performed therein.

Conflict of interest declaration. We declare we have no competing interests.

Acknowledgements. S.T. is funded by the NERC IAPETUS DTP (NE/S007431/1), supervised by S.M.W., C.A.C., B.V.P. and D.B. S.M.W., C.A.C. and D.B. were supported by EPSRC (EP/Y017838/1) and EPSRC (EP/Y017919/1). S.M.W. and D.B. were supported by BBSRC-Defra (BB/X018113/1). The funding sources had no role in study design; in the collection, analysis and interpretation of data; in the writing of the report; and in the decision to submit the paper for publication.

References

1. Roiz D *et al*. 2024 The rising global economic costs of invasive *Aedes* mosquitoes and *Aedes*-borne diseases. *Sci. Total Environ*. **933**, 173054. (doi:10.1016/j.scitotenv.2024.173054)
2. Laiton-Donato K, Guzmán-Cardozo C, Peláez-Carvajal D, Ajami NJ, Navas MC, Parra-Henao G, Usme-Ciro JA. 2023 Evolution and emergence of mosquito-borne viruses of medical importance: towards a routine metagenomic surveillance approach. *J. Trop. Ecol*. **39**, e13. (doi:10.1017/s0266467423000019)
3. Constant LEC, Rajsfus BF, Carneiro PH, Sisnande T, Mohana-Borges R, Allonso D. 2021 Overview on chikungunya virus infection: from epidemiology to state-of-the-art experimental models. *Front. Microbiol*. **12**, 744164. (doi:10.3389/fmicb.2021.744164)
4. World Health Organization. 2022 Chikungunya. See https://www.who.int/news-room/fact-sheets/detail/chikungunya.
5. European Centre for Disease Prevention and Control. 2024 Communicable disease threats report, 16-22 November 2024, week 47. See https://www.ecdc.europa.eu/sites/default/files/documents/Communicable-disease-threats-report-week-47-2024.pdf.
6. European Centre for Disease Prevention and Control. 2024 Aedes albopictus - current known distribution: May 2024. See https://www.ecdc.europa.eu/en/publications-data/aedes-albopictus-current-known-distribution-may-2024.

7. European Centre for Disease Prevention and Control. 2024 Local transmission of chikungunya virus in mainland EU/EEA, 2007–present. See https://www.ecdc.europa.eu/en/infectious-disease-topics/chikungunya-virus-disease/surveillance-threats-and-outbreaks/local.
8. Liu-Helmersson J, Quam M, Wilder-Smith A, Stenlund H, Ebi K, Massad E, Rocklöv J. 2016 Climate change and *Aedes* vectors: 21st century projections for dengue transmission in Europe. *EBioMedicine* **7**, 267–277. (doi:10.1016/j.ebiom.2016.03.046)
9. European Centre for Disease Prevention and Control. 2024 Factsheet for health professionals about chikungunya. See https://www.ecdc.europa.eu/en/chikungunya/facts/factsheet.
10. Medlock JM, Leach SA. 2015 Effect of climate change on vector-borne disease risk in the UK. *Lancet Infect. Dis*. **15**, 721–730. (doi:10.1016/S1473-3099(15)70091-5)
11. Jourdain F *et al*. 2020 From importation to autochthonous transmission: drivers of chikungunya and dengue emergence in a temperate area. *PLoS Neglected Trop. Dis*. **14**, e0008320. (doi:10.1371/journal.pntd.0008320)
12. Christofferson RC, Turner EA, Peña-García VH. 2023 Identifying knowledge gaps through the systematic review of temperature-driven variability in the competence of *Aedes aegypti* and *Ae. albopictus* for chikungunya virus. *Pathogens* **12**, 1368. (doi:10.3390/pathogens12111368)
13. Ohm JR, Baldini F, Barreaux P, Lefevre T, Lynch PA, Suh E, Whitehead SA, Thomas MB. 2018 Rethinking the extrinsic incubation period of malaria parasites. *Parasit. Vectors* **11**, 178. (doi:10.1186/s13071-018-2761-4)
14. Lahondère C, Bonizzoni M. 2022 Thermal biology of invasive *Aedes* mosquitoes in the context of climate change. *Curr. Opin. Insect Sci*. **51**, 100920. (doi:10.1016/j.cois.2022.100920)
15. Zardini A *et al*. 2024 Estimating the potential risk of transmission of arboviruses in the Americas and Europe: a modelling study. *Lancet Planet. Health* **8**, e30–e40. (doi:10.1016/S2542-5196(23)00252-8)
16. Lühken R *et al*. 2024 High vector competence for chikungunya virus but heavily reduced locomotor activity of *Aedes albopictus* from Germany at low temperatures. *Parasit. Vectors* **17**, 502. (doi:10.1186/s13071-024-06594-x)
17. Heitmann A, Jansen S, Lühken R, Helms M, Pluskota B, Becker N, Kuhn C, Schmidt-Chanasit J, Tannich E. 2018 Experimental risk assessment for chikungunya virus transmission based on vector competence, distribution and temperature suitability in Europe, 2018. *Eurosurveillance* **23**, 1800033. (doi:10.2807/1560-7917.es.2018.23.29.1800033)
18. Fischer D, Thomas SM, Suk JE, Sudre B, Hess A, Tjaden NB, Beierkuhnlein C, Semenza JC. 2013 Climate change effects on chikungunya transmission in Europe: geospatial analysis of vector's climatic suitability and virus' temperature requirements. *Int. J. Health Geogr*. **12**, 51. (doi:10.1186/1476-072X-12-51)
19. Tjaden NB, Cheng Y, Beierkuhnlein C, Thomas SM. 2021 Chikungunya beyond the tropics: where and when do we expect disease transmission in Europe? *Viruses* **13**. (doi:10.3390/v13061024)
20. Mordecai EA *et al*. 2017 Detecting the impact of temperature on transmission of Zika, dengue, and chikungunya using mechanistic models. *PLoS Negl. Trop. Dis*. **11**, e0005568. (doi:10.1371/journal.pntd.0005568)
21. Johansson MA, Powers AM, Pesik N, Cohen NJ, Staples JE. 2014 Nowcasting the spread of chikungunya virus in the Americas. *PLoS One* **9**, e104915. (doi:10.1371/journal.pone.0104915)
22. Vega-Rúa A *et al*. 2015 Chikungunya virus transmission potential by local *Aedes* mosquitoes in the Americas and Europe. *PLoS Negl. Trop. Dis*. **9**, e0003780. (doi:10.1371/journal.pntd.0003780)
23. Tsetsarkin KA, Vanlandingham DL, McGee CE, Higgs S. 2007 A single mutation in chikungunya virus affects vector specificity and epidemic potential. *PLoS Pathog*. **3**, e201. (doi:10.1371/journal.ppat.0030201)
24. Tesla B, Demakovsky LR, Mordecai EA, Ryan SJ, Bonds MH, Ngonghala CN, Brindley MA, Murdock CC. 2018 Temperature drives Zika virus transmission: evidence from empirical and mathematical models. *Proc. R. Soc. B Biol. Sci*. **285**, 20180795. (doi:10.1098/rspb.2018.0795)
25. Shocket MS, Verwillow AB, Numazu MG, Slamani H, Cohen JM, El Moustaid F, Rohr J, Johnson LR, Mordecai EA. 2020 Transmission of West Nile and five other temperate mosquito-borne viruses peaks at temperatures between 23°C and 26°C. *eLife* **9**, e58511. (doi:10.7554/eLife.58511)
26. Mordecai EA *et al*. 2013 Optimal temperature for malaria transmission is dramatically lower than previously predicted. *Ecol. Lett*. **16**, 22–30. (doi:10.1111/ele.12015)
27. Mordecai EA *et al*. 2019 Thermal biology of mosquito-borne disease. *Ecol. Lett*. **22**, 1690–1708. (doi:10.1111/ele.13335)
28. Brass DP, Cobbold CA, Purse BV, Ewing DA, Callaghan A, White SM. 2024 Role of vector phenotypic plasticity in disease transmission as illustrated by the spread of dengue virus by *Aedes albopictus*. *Nat. Commun*. **15**, 7823. (doi:10.1038/s41467-024-52144-5)
29. PubMed. 2024 National library of medicine 2024. See https://pubmed.ncbi.nlm.nih.gov/.
30. Scopus. 2024 Scopus: empowering research with the world's leading abstract and citation database. See https://www.scopus.com/search/form.uri?display=basic#basic.
31. Moher D, Liberati A, Tetzlaff J, Altman DG. 2009 Preferred reporting items for systematic reviews and meta-analyses: the PRISMA statement. *PLoS Med.* **6**, e1000097. (doi:10.1371/journal.pmed.1000097)
32. Yu-Sung S, Masanao Y, Gianluca B. 2008 R2jags: using R to run 'JAGS'. 0.8-9. *R Core Team*. See https://cran.r-project.org/web/packages/R2jags/R2jags.pdf.
33. Ngumbang J, Meredith M, Kruschke J. 2024 HDInterval: highest (posterior) density intervals. 0.2.4. *R Core Team*. See https://cran.r-project.org/web/packages/HDInterval/HDInterval.pdf.
34. Shapiro LLM, Whitehead SA, Thomas MB. 2017 Quantifying the effects of temperature on mosquito and parasite traits that determine the transmission potential of human malaria. *PLoS Biol*. **15**, e2003489. (doi:10.1371/journal.pbio.2003489)
35. Tjørve KMC, Tjørve E. 2017 The use of Gompertz models in growth analyses, and new Gompertz-model approach: an addition to the Unified-Richards family. *PLoS One* **12**, e0178691. (doi:10.1371/journal.pone.0178691)
36. Real LA. 1977 The kinetics of functional response. *Am. Nat*. **111**, 289–300. (doi:10.1086/283161)
37. Detinova TS, BertramDS, World Health Organization. 1962 *Age-grouping methods in diptera of medical importance, with special reference to some vectors of malaria / T. S. Detinova ; [with] an annex on the ovary and ovarioles of mosquitos (with glossary) by D. S. Bertram*. Geneva, Switzerland: World Health Organization. (doi:10.2307/3275215)
38. Brady OJ *et al*. 2014 Global temperature constraints on *Aedes aegypti* and *Ae. albopictus* persistence and competence for dengue virus transmission. *Parasit. Vectors* **7**, 338. (doi:10.1186/1756-3305-7-338)
39. Gillooly JamesF, Charnov EL, West GB, Savage VM, Brown JH. 2002 Effects of size and temperature on developmental time. *Nature* **417**, 70–73. (doi:10.1038/417070a)
40. Brown JH, Gillooly JF, Allen AP, Savage VM, West GB. 2004 Toward a metabolic theory of ecology. *Ecology* **85**, 1771–1789. (doi:10.1890/03-9000)
41. Parham PaulE, Michael E. 2010 Modeling the effects of weather and climate change on malaria transmission. *Environ. Health Perspect*. **118**, 620–626. (doi:10.1289/ehp.0901256)
42. Heffernan JM, Smith RJ, Wahl LM. 2005 Perspectives on the basic reproductive ratio. *J. R. Soc. Interface* **2**, 281–293. (doi:10.1098/rsif.2005.0042)
43. Dietz K. 1993 The estimation of the basic reproduction number for infectious diseases. *Stat. Methods Med. Res*. **2**, 23–41. (doi:10.1177/096228029300200103)
44. Hollingsworth TD, Pulliam JRC, Funk S, Truscott JE, Isham V, Lloyd AL. 2015 Seven challenges for modelling indirect transmission: vector-borne diseases, macroparasites and neglected tropical diseases. *Epidemics* **10**, 16–20. (doi:10.1016/j.epidem.2014.08.007)

45. ECMWF. 2024 ERA5-Land hourly data from 1950 to present: European centre for medium-range weather forecasts. See https://cds.climate.copernicus.eu/datasets/reanalysis-era5-land?tab=overview.
46. Tegar S. 2025 sandeeptegar/chikungunya_EIP_R0: release v1.0.0 - Code for chikungunya EIP and transmission in Europe (v1.0.0). Zenodo. (doi:10.5281/zenodo.15296661)
47. Suh E, Stopard IJ, Lambert B, Waite JL, Dennington NL, Churcher TS, Thomas MB. 2024 Estimating the effects of temperature on transmission of the human malaria parasite, *Plasmodium falciparum*. *Nat. Commun*. **15**, 3230. (doi:10.1038/s41467-024-47265-w)
48. Cattaneo P *et al*. 2025 Transmission of autochthonous Aedes-borne arboviruses and related public health challenges in Europe 2007–2023: a systematic review and secondary analysis. *Lancet Reg. Health Eur*. **51**, 101231. (doi:10.1016/j.lanepe.2025.101231)
49. Chan M, Johansson MA. 2012 The incubation periods of dengue viruses. *PLoS One* **7**, e50972. (doi:10.1371/journal.pone.0050972)
50. Moore PR, Johnson PH, Smith GA, Ritchie SA, Van Den Hurk AF. 2007 Infection and dissemination of dengue virus type 2 in *Aedes aegypti*, *Aedes albopictus*, and *Aedes scutellaris* from the Torres Strait, Australia. *J. Am. Mosq. Control Assoc*. **23**, 383–388. (doi:10.2987/5598.1)
51. Mariconti M, Obadia T, Mousson L, Malacrida A, Gasperi G, Failloux AB, Yen PS. 2019 Estimating the risk of arbovirus transmission in Southern Europe using vector competence data. *Sci. Rep*. **9**, 17852. (doi:10.1038/s41598-019-54395-5)
52. Dubrulle M, Mousson L, Moutailler S, Vazeille M, Failloux AB. 2009 Chikungunya virus and *Aedes* mosquitoes: saliva is infectious as soon as two days after oral infection. *PLoS One* **4**, e5895. (doi:10.1371/journal.pone.0005895)
53. Vega-Rua A, Zouache K, Caro V, Diancourt L, Delaunay P, Grandadam M, Failloux AB. 2013 High efficiency of temperate *Aedes albopictus* to transmit chikungunya and dengue viruses in the southeast of France. *PLoS One* **8**, e59716. (doi:10.1371/journal.pone.0059716)
54. Tsetsarkin KA, Weaver SC. 2011 Sequential adaptive mutations enhance efficient vector switching by chikungunya virus and its epidemic emergence. *PLoS Pathog*. **7**, e1002412. (doi:10.1371/journal.ppat.1002412)
55. Paaijmans KP, Blanford S, Chan BHK, Thomas MB. 2012 Warmer temperatures reduce the vectorial capacity of malaria mosquitoes. *Biol. Lett*. **8**, 2011. (doi:10.1098/rsbl.2011.1075)
56. Ruel JJ, Ayres MP. 1999 Jensen's inequality predicts effects of environmental variation. *Trends Ecol. Evol*. **14**, 361–366. (doi:10.1016/s0169-5347(99)01664-x)
57. Denny M. 2017 The fallacy of the average: on the ubiquity, utility and continuing novelty of Jensen's inequality. *J. Exp. Biol*. **220**, 139–146. (doi:10.1242/jeb.140368)
58. Wallinga J, Lipsitch M. 2006 How generation intervals shape the relationship between growth rates and reproductive numbers. *Proc. R. Soc. B* **274**, 599–604. (doi:10.1098/rspb.2006.3754)
59. European Centre for Disease Prevention and Control. 2024 Factsheet for health professionals about dengue. See https://www.ecdc.europa.eu/en/dengue-fever/facts.
60. European Centre for Disease Prevention and Control. 2024 Chikungunya contracted during travel: likely places of infection reported by travellers to the EU/EEA. See https://www.ecdc.europa.eu/en/chikungunya-virus-disease/surveillance/travel-associated-cases.
61. Zouache K, Fontaine A, Vega-Rua A, Mousson L, Thiberge JM, Lourenco-De-Oliveira R, Caro V, Lambrechts L, Failloux AB. 2014 Three-way interactions between mosquito population, viral strain and temperature underlying chikungunya virus transmission potential. *Proc. R. Soc. B Biol. Sci*. **281**, 20141078. (doi:10.1098/rspb.2014.1078)
62. Copernicus Climate Change Service (C3S). 2019 ERA5-Land hourly data from 1950 to present. Copernicus Climate Change Service (C3S) Climate Data Store (CDS) (doi:10.24381/cds.e2161bac)
63. Tegar S, Brass D, Purse BV, Cobbold CA, White SM. 2026 Supplementary material from: Temperature-sensitive incubation, transmissibility, and risk of Aedes albopictus-borne chikungunya virus in Europe. Figshare. (doi:10.6084/m9.figshare.c.8230348)